International Journal of Applied Earth Observation and Geoinformation 34 (2015) 25–34

Contents lists available at ScienceDirect

International Journal of Applied Earth Observation and Geoinformation

journal homepage: www.elsevier.com/locate/jag

Grassland habitat mapping by intra-annual time series analysis – Comparison of RapidEye and TerraSAR-X satellite data

Christian Schuster[a,b,*], Tobias Schmidt[b], Christopher Conrad[c], Birgit Kleinschmit[b], Michael Förster[b]

[a] Geoinformation Science Lab, Geography Department, Humboldt-Universität zu Berlin, Unter den Linden 6, 10099 Berlin, Germany
[b] Geoinformation in Environmental Planning Lab, Technische Universität Berlin, Straße des 17. Juni 145, 10623 Berlin, Germany
[c] Department of Remote Sensing, Department of Geography and Geology, Julius-Maximilians-Universität Würzburg, Oswald-Külpe-Weg 86, 97074 Würzburg, Germany

ARTICLE INFO

Article history:
Received 30 November 2013
Accepted 12 June 2014
Available online 23 July 2014

Keywords:
Natura 2000
Semi-natural grassland habitats
RapidEye
TerraSAR-X
Time series
Feature selection

ABSTRACT

Remote sensing concepts are needed to monitor open landscape habitats for environmental change and biodiversity loss. However, existing operational approaches are limited to the monitoring of European dry heaths only. They need to be extended to further habitats. Thus far, reported studies lack the exploitation of intra-annual time series of high spatial resolution data to take advantage of the vegetations' phenological differences. In this study, we investigated the usefulness of such data to classify grassland habitats in a nature reserve area in northeastern Germany. Intra-annual time series of 21 observations were used, acquired by a multi-spectral (RapidEye) and a synthetic aperture radar (TerraSAR-X) satellite system, to differentiate seven grassland classes using a Support Vector Machine classifier. The classification accuracy was evaluated and compared with respect to the sensor type – multi-spectral or radar – and the number of acquisitions needed. Our results showed that very dense time series allowed for very high accuracy classifications (>90%) of small scale vegetation types. The classification for TerraSAR-X obtained similar accuracy as compared to RapidEye although distinctly more acquisitions were needed. This study introduces a new approach to enable the monitoring of small-scale grassland habitats and gives an estimate of the amount of data required for operational surveys.

Introduction

To cope with environmental change and biodiversity loss, planning authorities need tools to monitor environmental habitats. A current major challenge is the improved integration of remote sensing into ecological research to enhance the measurement of changes in ecosystem diversity at local and global levels (Scholes et al., 2008; Naeem et al., 2012). A major driver in this respect has recently been the European Union Habitats Directive (European Commission, 2005) and the subsequent establishment of the pan European Natura 2000 network of nature protection sites. According to §7 European regional authorities are legally obligated to report on the status and extent of such sites in six-year intervals. To meet the demand for appropriate monitoring techniques, remote sensing options are explicitly requested and increasingly investigated by researchers (Bock et al., 2005; Vanden Borre et al., 2011). For forest habitats several successful approaches exist (e.g., Foerster et al., 2008); however, developed (and operationally available) concepts for mapping and updating open landscape habitat information are limited to European dry heaths only (Chan et al., 2012; Spanhove et al., 2012; Morán-Ordónez et al., 2012). New approaches need to be developed to extend remote sensing based monitoring concepts to further habitats.

Grasslands represent one of the largest managed landscape units in the terrestrial system. As such, they are essential contributors to global biodiversity. They are directly affected by the increasing competition of land use for food or energy production and for environmental benefits (Tilman et al., 2009). Grassland and grassland biodiversity faced a dramatic decline over the last decades (Klimek et al., 2007; Sullivan et al., 2010; Wright and Wimberly, 2013). Therefore, area-wide inventories and monitoring capacities are needed, beyond the frame of Natura 2000 (Scholes et al., 2008; De Bello et al., 2010).

* Corresponding author at: Geoinformation Science Lab, Geography Department, Humboldt-Universität zu Berlin, Unter den Linden 6, 10099 Berlin, Germany. Tel.: +49 30 2093 9380; fax: +49 30 2093 6848.
E-mail addresses: christian.schuster@geo.hu-berlin.de, chr.schuster@gmail.com (C. Schuster).

http://dx.doi.org/10.1016/j.jag.2014.06.004
0303-2434/

Grassland mapping, though, is a difficult task, in particular, when native or semi-natural habitats are concerned. The capacity to differentiate individual grassland habitat classes using remote sensing data is not reported. Despite recent successful attempts, even the mapping of differently managed grassland types is still regarded as challenging (Hill et al., 2005; Bock et al., 2005; Sullivan et al., 2010; Prishchepov et al., 2012; Franke et al., 2012; Wright and Wimberly, 2013). More sophisticated approaches for grassland mapping need to be developed, compared to relatively homogeneous agricultural areas, which have been more commonly targeted in remote sensing maps. The particular challenge is (a) in the small spatial extent of such habitats, (b) in their spectral similarity and (c) in the high spatial, structural and temporal diversity of the vegetation composition (Mehner et al., 2004; Hill et al., 2005; Schmidtlein et al., 2007; Schuster et al., 2011; Wright and Wimberly, 2013; Feilhauer et al., 2013). To cope with the spatial diversity, high ground resolutions are required (Franke et al., 2012; Feilhauer et al., 2013). Structural diversity could be observable using synthetic aperture radar (SAR) data. Provided that the employed sensors are sufficiently sensitive to capture such habitat differences, the temporal diversity might even be the key issue for a mapping solution: it theoretically allows for the discrimination of habitats via the distinction of different vegetation growth phases (Schmidtlein et al., 2007; Schuster et al., 2011; Atzberger, 2013).

The primary challenge for mapping fine scale grassland habitats therefore is to acquire intra-annual time series of both high spatial and high temporal resolution satellite data of relevant spectral sensitivity. Traditionally, though, remote sensing studies have to face an initial trade-off in the selection of either high spatial or high temporal resolution data (Lambin and Linderman, 2006). Clearly, using time series of satellite data to classify vegetation has been the topic of many surveys in the past, particularly as the temporal capabilities of satellite systems steadily improve (Justice and Hiernaux, 1983; Zhang et al., 2003; Atzberger and Eilers, 2011). Until recently, multitemporal remote sensing of vegetation has been a domain of spatial coarse scale (250 m to 1 km) optical sensors, such as NOAA AVHRR, TERRA MODIS, ENVISAT MERIS or SPOT VEGETATION (Hill et al., 1999; Zhang et al., 2003; Fontana et al., 2008; Gu et al., 2010; Jacquin et al., 2010; Boyd et al., 2011; Conrad et al., 2011; Lhermitte et al., 2011; Alcantara et al., 2012; Ullah et al., 2012; Atzberger and Eilers, 2011). With the development of multi-sensor satellite systems such as RapidEye or future Sentinel-2, however, the temporal resolution of high spatial resolution optical sensors is increasing remarkably. RapidEye data has been successfully applied to classify vegetation units or canopy nitrogen using single-date approaches (Schuster et al., 2012b; Ramoelo et al., 2012). Multitemporal RapidEye data sets showed notable benefits to classify area-wide vegetation details (Conrad et al., 2012; Franke et al., 2012; Tigges et al., 2013). To test if intra-annual time series of optical high resolution data allows classifying heterogeneous semi-natural grassland habitats, we acquired an exceptionally dense series of cloud-free RapidEye imagery.

While optical satellite data has been the traditional basis for vegetation surveys, synthetic aperture radar (SAR) systems are advancing in this domain. The principal advantage of SAR sensors is their all-weather capability, so that the acquisition of steady time series is not hampered by frequent cloud coverage. They collect information on the height and structure of vegetation, in contrast to optical data, which is sensitive to chemical leaf composition. Several previous reported SAR studies indicated the potential benefit of analyzing SAR data to differentiate vegetation (Price et al., 2002; Moreau and Le Toan, 2003; Hill et al., 2005; Baghdadi et al., 2009; Hadria et al., 2010; Evans and Costa, 2013). Nevertheless, recent spaceborn C-band (Envisat-ASAR, Radarsat-2) or L-band (ALOS PALSAR) systems have not been sufficiently sensitive for grassland mapping. Due to the relatively long electro-magnetic microwaves and low spatial resolutions, previous studies did not achieve proper classification of heterogeneous grassland patterns (Hill et al., 1999; Price et al., 2002; Hill et al., 2005). Moreover, none of them are concerned with time series data, although multitemporal steadiness is commonly regarded as the major advantage of SAR systems.

The TerraSAR-X system has brought many new opportunities in terms of spatial resolution and signal sensitivity. It provides the sensitive X-band and high spatial resolution data for the first time in an operational space-born SAR-system. Thus, it has made the sensing of finer vegetation structures possible (Lopez-Sanchez et al., 2010; Baghdadi et al., 2010; Bargiel and Herrmann, 2011; Schuster et al., 2011; Esch et al., 2011; Bargiel, 2013). TerraSAR-X data can be ordered in steady 11-day period with constant sensor configuration. Therefore, we acquired a very dense and homogenous intra-annual time series. We demonstrated its usability for investigating the temporal development of highly–variably composited semi-natural grassland vegetation (Schuster et al., 2011, 2012a). However, can we also use that data for pixel-based classifications of grassland habitats?

The ultimate goal of this study is to test if the use of intra-annual time series of high spatial resolution satellite data enables to successfully classify fine-scaled and heterogenous grassland habitats. We generate intra-annual time series from satellite systems which are capable of delivering both high spatial and high temporal resolution data: RapidEye and TerraSAR-X. We investigate if the acquired time series allow differentiating seven habitat types using a Support Vector Machine (SVM) as well-established classification algorithm. Our approach intends to compare the systems with respect to the maximum classification accuracy reached, and the number of acquisitions needed to provide sufficient quality for monitoring applications.

Methods

Study site

The study site is part of the Döberitzer Heide, a nature protection site west of Berlin, the capital of Germany. It extents over 60 km^2 from 52.54° N/12.98° E to 52.46° N/13.10° E. The landscape is dominated by woodland. As former military training area, it also comprises large sections of open landscape. It represents a rich semi-natural landscape mosaic with various small-scale vegetation habitats. Dry sandy heaths, semi-natural grasslands, humid meadows, and wetlands dominate the flat open landscape. Many species-rich habitats, including highly endangered Natura 2000 habitats, are present. Therefore, interest in testing remote sensing monitoring tools arises beyond the frame of the EU Habitats Directive (European Commission, 2005). Remote sensing approaches are also needed since large sections of the area are inaccessible due to remnants of military munitions. In accordance with the common area coverage from both satellite tracks, the closer research area of this study is situated in the northwestern part of the Döberitzer Heide, mainly covering the humid meadow sections of the Ferbitzer Bruch (Fig. 1).

Optical and radar time series

This study is based on RapidEye and TerraSAR-X. Both systems are capable of providing both high spatial and high temporal resolution data. From each system, 21 scenes were acquired for the study site. Fig. 2 illustrates the information content of respective single scenes.

The optical Earth observation system RapidEye provides a ground resolution of 6.5 m at nadir. It is designed as constellation of five mini-satellites in sun-synchronous orbit. Thus, the

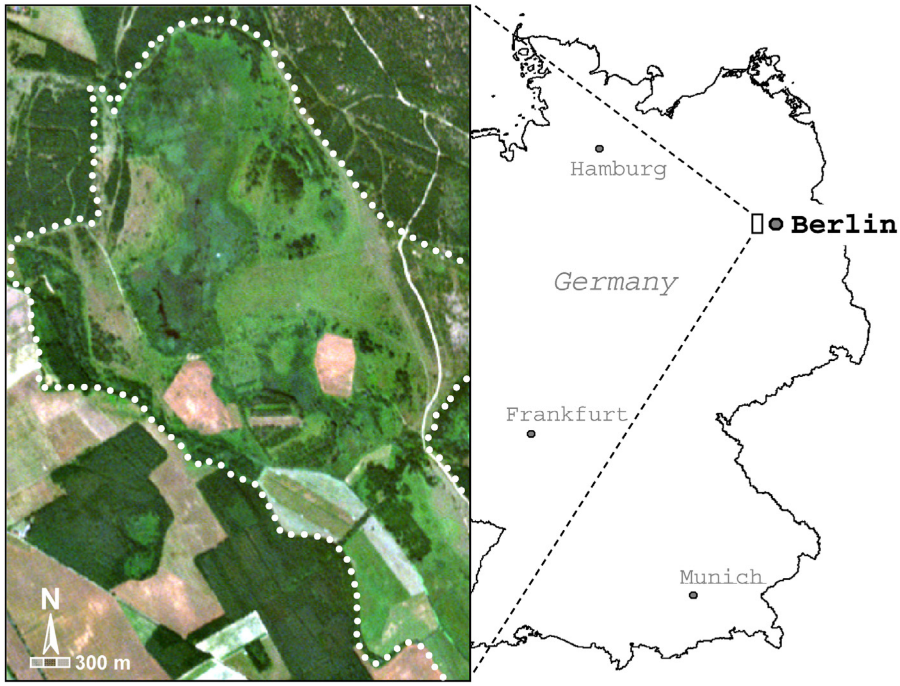

Fig. 1. The study site west of Berlin, as seen in a RapidEye true color image subset from July 27th 2009. (For interpretation of the references to color in text, the reader is referred to the web version of this article.)

system is capable of delivering comparatively high frequency revisits of theoretically 5.5 days at nadir with a constant look angle (RapidEye, 2012). Apart from common sensor limitations (on board storage capacity, etc.), the actually achievable temporal resolution rate is significantly reduced due to cloud coverage. Nevertheless, we finally received a very large time series of 21 rather cloud-free scenes collected during the main vegetation periods (March to October) between 2009 and 2011. RapidEye data products are multi-spectral, recorded in five optical bands in the 400–850 nm range (blue, green, red, red-edge, near infra red) in 12 bit dynamic range. The additionally delivered red-edge band appears particularly suitable for vegetation mapping (Conrad et al., 2012; Schuster et al., 2012b). Imagery of the research area is recorded at approximately 11 a.m. daily. The data were ordered in level 1B (basic geometric and radiometric corrections; RapidEye, 2012) in order to achieve higher radiometric and geometric accuracy than that provided by the standard level 3A product.

The pre-processing began with the production of geometric image subsets by manual extraction from the study area. Each image was then geo-rectified based on a Quickbird scene

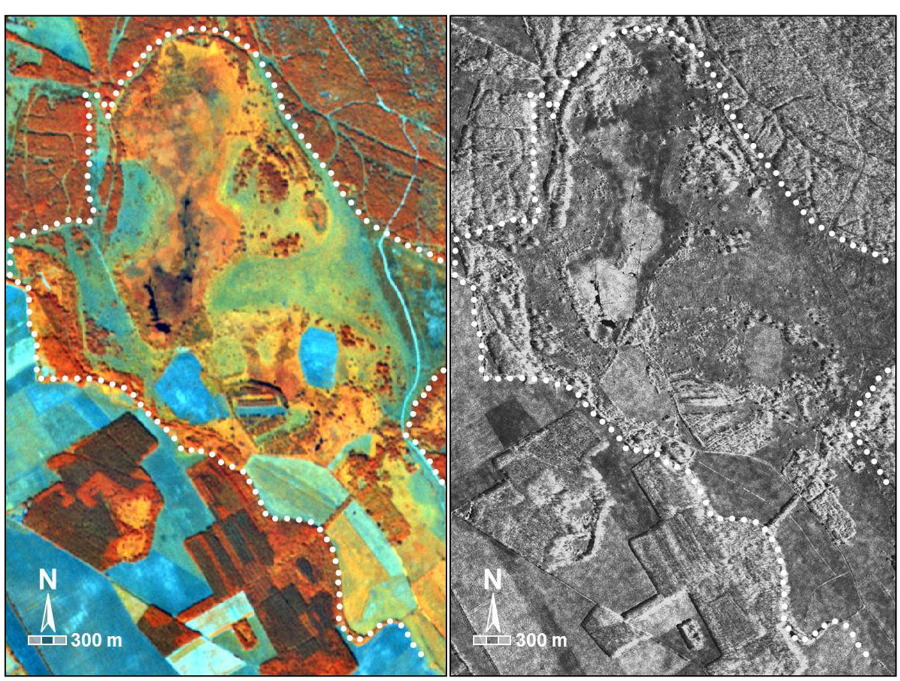

Fig. 2. Single date acquisition for RapidEye (2009-07-27, color – red edge composition) and TerraSAR-X (2010-07-27, single band gray scale). (For interpretation of the references to color in text, the reader is referred to the web version of this article.)

Table 1
Acquisition distribution over the year RapidEye and TerraSAR-X, indicated by date, day of year (DoY), and the temporal distance to the previous acquisition. The distribution for RapidEye, phenologically corrected and integrated into an artificial one-year series, is still quite uneven, while the TerraSAR-X series features an almost constant 11-day period.

Acquisition date	DoY[a]	RapidEye Temporal distance to previous acquisition	TerraSAR-X Temporal distance to previous acquisition	DoY	Acquisition date
2011-03-24	79			65	2010-03-06
2009-04-03	94	15	11	76	2010-03-17
2011-04-21	111	17	11	87	2010-03-28
2011-05-06	129	18	11	98	2010-04-08
2010-05-26	139	10	22	120	2010-04-30
2010-06-04	147	8	22	142	2010-05-22
2009-05-24	155	8	11	153	2010-06-02
2011-05-30	158	3	11	164	2010-06-13
2011-06-04	164	6	11	175	2010-06-24
2010-06-27	170	6	11	186	2010-07-05
2010-07-08	182	12	11	197	2010-07-16
2010-07-16	191	9	11	208	2010-07-27
2009-07-27	216	25	11	219	2010-08-07
2010-08-21	234	18	11	230	2010-08-18
2009-08-19	236	2	11	241	2010-08-29
2009-09-20	267	31	11	252	2010-09-09
2011-09-26	269	2	11	263	2010-09-20
2010-09-22	273	4	33	296	2010-10-23
2010-10-04	285	12	11	307	2010-11-03
2011-10-22	295	10	11	318	2010-11-14
2009-10-19	297	2	11	329	2010-11-25

[a] Phenologically corrected.

(1 m resolution) to obtain sub-pixel spatial accuracy using 25 ground control points and 2nd order polynomial coefficients, and projected to ETRS 1989, UTM 33N. Due to the flat terrain of the study site, no terrain related corrections were performed. Next, all images were atmospherically corrected using the Erdas Imagine ATCOR 2 tool (Richter, 1996). Only five images were affected by cloud cover at all. The remaining minimal cloud and cloud shadow areas (each covering up to 2% of the study site area) were masked out.

As is commonly done in optical time series analysis (e.g., Alcantara et al., 2012; Jacquin et al., 2010; Zhang et al., 2003; Esch et al., 2014), the vegetation index NDVI was calculated to estimate the vegetation's greenness and photosynthetic activity by area (Tucker, 1979). As previous studies reported an increase in classification accuracy for the RapidEye red-edge band when used for observation of open landscape vegetation (Conrad et al., 2012; Schuster et al., 2012b; Ramoelo et al., 2012), this study was extended on red-edge based adaptations of the classic NDVI. Two further indices were calculated: (a) the NDVI Red-Edge–Red (NDVI-RE-R) where the NIR band is substituted by the red-edge band (Souza et al., 2010; Schuster et al., 2012b) and (b) the NDVI NIR–Red-Edge (NDVI-NIR-RE) (Gitelson and Merzlyak, 1994; Sims and Gamon, 2002) where the red band is replaced by the red-edge band.

To achieve a rather dense and relatively homogenous intra-annual time series, the individual dates of acquisition, spanning over three vegetation periods from April 2009 to September 2011, were phenologically corrected with respect to the target year, 2010. Therefore, long-term phenological observation data from the German National Meteorological Service (DWD) were used to reallocate the images as introduced by Foerster et al. (2012). The corrected data were ordered according to their phenological date (Table 1) and integrated into one NDVI, one NDVI-RE-R, and one NDVI-NIR-RE layer stack. Temporal gaps resulting from the cloud mask were substituted by linear interpolation using the previous and the following pixel in the time series.

Due to the radar system's independence from cloud interference, it was much easier to achieve a dense and continuous time series with TerraSAR-X than with RapidEye. The TerraSAR-X series consists of 21 scenes all acquired during the vegetation growing period in 2010. It represents an almost continuous and truly equidistant 11-day time series with few exceptions (Table 1). All data are recorded in X-band (∼3 cm wavelength), HH-polarization and strip map imaging mode with a spatial resolution of 3 m in ground range and 3.3 m in azimuth direction. They were acquired at 5:33 a.m. from the same satellite track (orbit 78) with a constant incidence angle of 27.9°. The scenes were ordered partly pre-processed as enhanced ellipsoid corrected (EEC) ground range level 1B products, with equidistant pixel spacing in azimuth and ground range direction. To complement the small habitat spatial extents, high geometric precision was targeted by ordering the data in 'high orbit precision' (Infoterra, 2008; Breit et al., 2010).

To match the spatial pixel size of the RapidEye data, the scenes were sampled to 6.5 m pixel size during the process of image co-registration. After co-registration, the multitemporal DeGrandi filtering (Jong-Sen et al., 1999), as implemented in the ENVI SARSCAPE 4.5 software package, was performed on all images to reduce radar speckle. Next, the individual scenes were layer stacked and geometric image subsets of the study area were extracted. In contrast to the individual application used for each of the RapidEye scenes, the geo-rectification process could be performed for the entire stack. Analogous to the RapidEye data, a sub-pixel spatial accuracy was achieved based on the use of a Quickbird scene (1 m resolution), and terrain corrections were not performed. The geo-rectification was done using 21 ground control points and 2nd order polynomial coefficients and projected to ETRS 1989, UTM 33N. The resulting layer stack was a backscatter intensity time series.

As final pre-processing steps, a mask was build to exclude forest and other non-grassland section of the research area from the classification process. Fig. 3 illustrates several results from pre-processing and indicates the information gain when several acquisition dates were overlaid.

Reference data

The semi-natural open landscape vegetation in the *Ferbitzer Bruch* research area was mapped to cover the full range of vegetation diversity. Grassland habitats, vegetation classes and dominant single plant types were determined according to respective state of

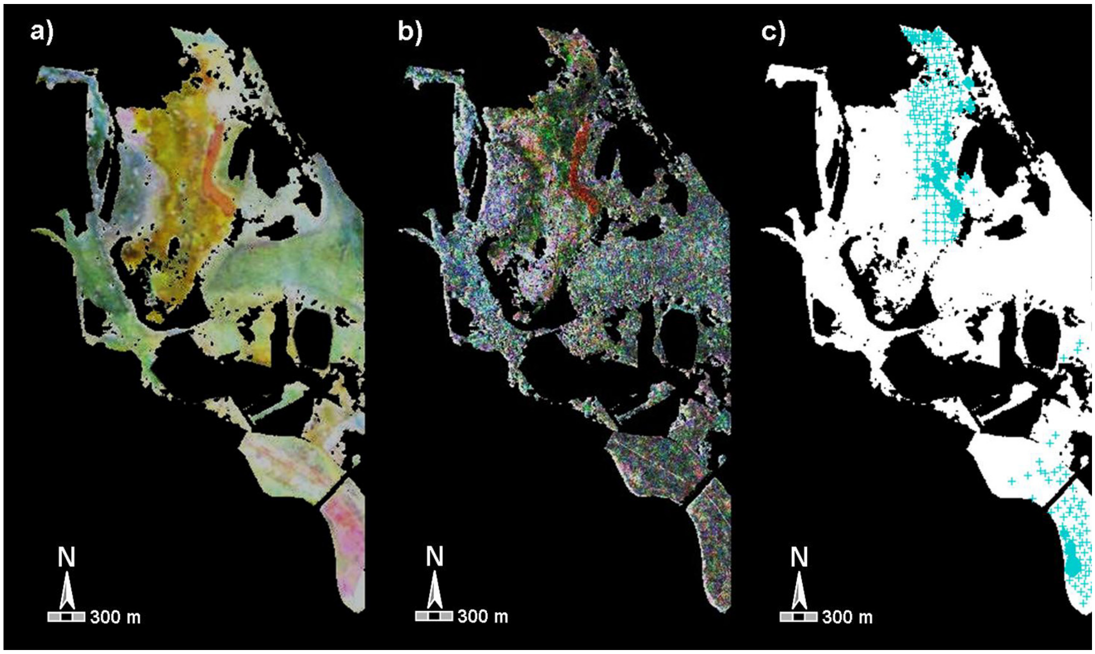

Fig. 3. Vegetation mask (black), time-series image overlays for (a) RapidEye and (b) TerraSAR-X, and (c) sampling spots (blue). Illustrated bands are for (a) RapidEye NDVI (red: 2010-08-21, green: 2009-07-27, blue: 2010-07-16) and for (b) TerraSAR-X backscatter (red: 2010-08-29, green: 2010-08-18, blue: 2010-08-07). (For interpretation of the references to color in text, the reader is referred to the web version of this article.)

the art literature (Dierschke, 1994; Rothmaler, 2000, 2005; Klapp and von Boberfeld, 1995). The mapping was performed primarily from May to June 2010 during the vegetations' maximum development phase, including frequent control visits to observe temporal ground dynamics, in particular human mowing impacts. Stratified sampling was done based on a pre-selection of suitable areas for sampling locations according to two main deliberations: first, the accessibility of sub-areas, limited by remnants of munitions and the swamp area, second, the aim to cover all vegetation types in the research area (Fig. 3).

Based on this area-wide mapping, the spatial delineation of habitat patches was optimized to meet the requirements for an image-based analysis of RapidEye 6.5 m resolution data. Therefore, individual patches should cover no less than an area of 3×3 pixels and add up to cover a minimum overall sample size of approximately 30 image pixels per habitat class to ensure sufficient training and validation pixels (Foody et al., 2006; Congalton and Green, 2009). Provided that they represented ecologically relatively homogenous areas of a size, the aggregation was performed according to the nomenclature of the §32 official biotope map of the federal state of Brandenburg, as described by Pott (1995) and Schubert et al. (2001). The resulting scenario to be classified includes seven grassland habitat classes, mainly humid meadow and partly wetland sections (Table 2). The investigated habitats represent an ideal study case since they comprise many perennial herbaceous plants with clear and dominant phenological development aspects.

Table 2
Investigated habitat classes (plant societies) and respective sample sizes (pixel size: 6.5 m).

Class No.	Plant society	Sample size (No. of pixels)
1	*Molinion caeruleae*	130
2	*Calthion palustris*	88
3	*Caricion elatae*	50
4	*Arrhenatheretum elatioris*	153
5	*Arrhenaterion elatioris*	30
6	*Solidago canadensis*	29
7	*Phragmitetum australis*	85

Permanent plots were established and regularly visited for a field spectrometry measurement survey for the time of data acquisition until September 2011. Thus, habitat conditions could be frequently observed and updated. Mowing activities as major change impacts were precisely recorded by the local area stakeholders and were apparent in the field.

Classification and feature assessment

Both data sets were classified using the Support Vector Machine (SVM) algorithm (Rabe et al., 2010b). SVMs represent a powerful method for the classification of remote sensing data. Over the last decade, several studies have shown that these machine-learning algorithms exceed the performance of established classifiers (Huang et al., 2002; van der Linden and Hostert, 2009; Schuster et al., 2012b; Baumann et al., 2012). SVM is a supervised non-parametric statistical learning technique. As a binary classifier, the SVM training algorithm separates two classes by using an optimal separating hyperplane to distinguish the training samples in a multidimensional feature space. This procedure is repeated for each pair of classes to divide the data into the predefined number of classes. Support vectors are the training samples that are located closely to the class borders; the hyperplane aims at maximizing the distance to them in a learning process of structural risk optimization. Apart from the high discrimination power in general, SVMs are particularly well-suited for classifications with only small training data sets and no underlying assumptions of statistical distribution (Foody and Mathur, 2004; Waske and Van der Linden, 2008; Mountrakis et al., 2010), which is of specific advantage in the context of this study.

The ground truth data sets deducted from the habitat classes mapped in the field (Table 2) were divided into training and validation data sets using stratified random sampling, thereby keeping 70% of each class sample for training and 30% for the validation. Classification accuracy was assessed using three different kinds of measure – overall accuracy (percentage of the correctly classified

Table 3
Classification accuracies for the TerraSAR-X and RapidEye time series – total averages (overall accuracy, Kappa coefficient, F_1 measure) and class-specific (F_1 measure).

Sensor	TerraSAR-X	RapidEye		
Index		*NDVI*	*NDVI-RE-R*	*NDVI-NIR-RE*
Overall accuracy (%)	91.1	91.7	89.9	91.7
Kappa coefficient	0.89	0.90	0.88	0.90
F_1 measure (%)	89.3	87.9	84.2	88.2
Molinion caeruleae	96	98	97	96
Calthion palustris	80	89	88	84
Caricion elatae	73	69	64	80
Arrhenatheretum elatioris	96	98	95	96
Arrhenaterion elatioris	94	80	71	80
Solidago canadensis	94	85	81	85
Phragmitetum australis	88	87	88	93

pixels in the validation dataset), the kappa coefficient of agreement (difference measure between the actual and the chance agreement) (Laurin et al., 2013), and the averaged F_1 measure as the harmonic mean of producer and user accuracy (Halder et al., 2009; Schuster et al., 2012b; Baumann et al., 2012). The latter is regarded as the more meaningful measure than the kappa coefficient and overall accuracy. However, these standard measures are incorporated to enhance the comparability with other remote sensing applications.

To investigate how many acquisitions are needed to optimize classification accuracy, the SVM-based forward feature selection (FFS) as implemented in imageSVM was used (Rabe et al., 2010b). Basically, it ranks the features of a feature stack according to their discriminant power by selecting relevant, non-redundant features via a stepwise forward selection (Kohavi and John, 1997). The process starts with selecting the most relevant feature for the given training and independent validation sample. Then, in the second iteration, SVMs are trained for each pair of features consisting of the best performing feature and one additional feature. In a five-fold 'forward selection' process, additional features are added according to their extra classification power – referring to the information content of the respective previously selected features. The increase in classification accuracy for each additional feature is documented in a learning curve (compare Fig. 3) (Rabe et al., 2010a; Griffiths et al., 2010; Tigges et al., 2013). While the actual ranking of features is not stable mainly due to the randomized selection process and redundancy problems, it returns a reliable estimation of the rise in classification accuracy for the subsequent integration of features into the classification process. Therefore, the learning curve can be interpreted in order to determine accuracy accumulation points, i.e., for deciding on relevant time series extents.

In remote sensing studies, no clearly defined levels exist for the evaluation of classification accuracy (Foody, 2008). For this evaluation, the accuracy accumulation is characterized by two observation marks: how many features are needed to obtain a classification accuracy level of 85% (F_1 measure)? Also, when is a relative saturation in accuracy reached, determined by 95% of the respective time series' highest (total) classification accuracy (F_1 measure)?

Results

Classification accuracy

The results for the classification show that the produced time series of both sensors can achieve very high classification accuracies of more than 90% overall accuracy (Table 3). The highest accuracies are obtained using the RapidEye NDVI-NIR-RE stack, closely followed by the TerraSAR-X stack and the NDVI-stack, depending on which accuracy measure is compared. Yet, these differences are marginal. The classification accuracy for TerraSAR-X, NDVI-NIR-RE, and the NDVI commonly reaches high accuracy values around 90% or 0.9 kappa coefficient, respectively. The NDVI-RE-R stack is slightly less accurate.

The best class-specific results are returned for the plant societies *Molinion caeruleae* and *Arrhenatheretum elatioris*, with accuracies above 95% for all feature stacks. Both are classified best using the NDVI. The lowest accuracies, 64–80%, occurred for *Caricion elatae*. The TerraSAR-X feature stack allows for distinctively higher class-specific classification accuracies for *Arrhenaterion elatioris*, with 94% compared to 70–80% for the RapidEye stacks, as well as for *Solidago canadensis*, with 94% compared to 81–85%. Vice versa, the RapidEye information content appears to be more valuable for the classification of *Calthion palustris*, returning 84–89% compared to 80% for the TerraSAR-X stack.

Scene number learning curve

All learning curves produced by the SVM Feature Subset Selection show a common general pattern. It is characterized by an initial rather steep increase, followed by a relatively continuous accumulation of classification accuracy on a high level with minor oscillations (Fig. 4). Yet, a clear difference is visible between the RapidEye and TerraSAR-X time series. While the asymptotic classification accuracies are rather similar, the RapidEye-stacks begin at a much higher initial (single-date) classification accuracy and gain the relative saturation level distinctly earlier. The RapidEye feature stacks' classification accuracy begins at approximately 40% with one scene, rises rather quickly to 60–70% with two images, and – for the NDVI-NIR-RE – reaches almost 80% with only three images. The 85% mark is broken with six (NDVI) or seven (NDVI-NIR-RE) scenes (while never quite obtained for the NDVI-RE-R-stack). The TerraSAR-X feature stack accuracy begins rather low with only 23% and barely reaches 60% with three scenes. It takes eight images to exceed the 80% level and 13 images to reach the 85% mark, before it finally obtains the same accuracy as the RapidEye stack. The overall increase in classification accuracy is relatively steady and more homogenous compared to the RapidEye stacks. Hence, 15 scenes are needed to approach 95% of the final accuracy in the TerraSAR-X stack, while for RapidEye only five features (six for the NDVI-RE-R) are needed to attain this level of accuracy.

Discussion – implications for grassland habitat mapping

The results demonstrate the potential of intra-annual high resolution time series for accurately classifying small-scale grassland

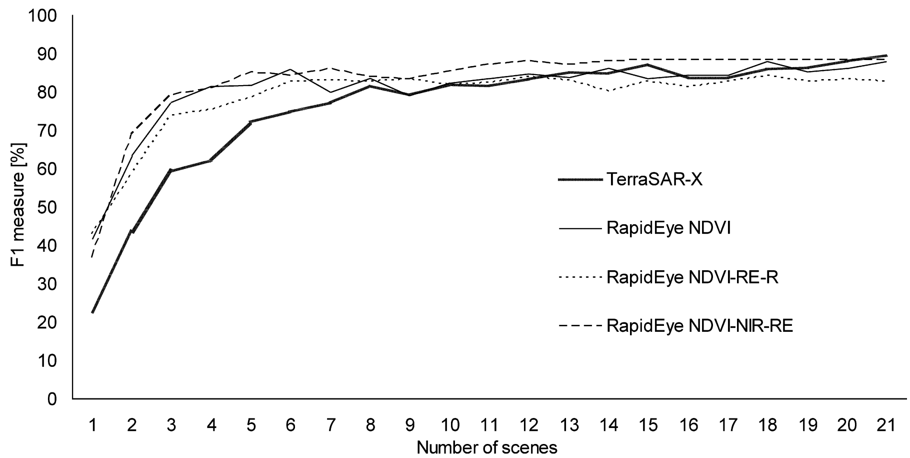

Fig. 4. Change in classification accuracy according to the number of scenes used. The X-axis shows the F_1 measure (%) for the rank (*Y*-axis) in the respective feature stack. Procedure: Feature forward selection, 5-folds, independent validation. Software: imageSVM (Rabe et al., 2010b).

habitats. To the best of our knowledge this is the first reported study to classify individual units of semi-natural grassland vegetation using satellite data. The high accuracy level holds for RapidEye data and to the same extent for TerraSAR-X time series.

Most certainly, the main reason is found in the characteristic phenological development of individual habitat classes. The evolution of greenness per area, supplemented by additional coloring aspect from different blossoming phases, supports the separability using dense intra-annual time series of optical data. The evolution of the vegetations' height and structure affects the radar backscatter over time. Such indicative characteristics are very much supported by the characteristical phenology of the perennial herbaceous plants with their annual regrowth of stems and distinct florescence. Moreover, the hay cut, as a major human impact, further influences the temporal signal evolution for both systems. These temporal effects seem to be sufficiently well captured by the presented approach for differentiation of individual habitat classes.

High spatial and temporal resolution

Joint high spatial and high temporal resolution appears to be a key system requirement to map small-scale vegetation habitats. Our study confirms the need for high spatial resolution optical data and repeated acquisitions during the vegetation period, as emphasized by Franke et al. (2012). Their study reports an overall accuracy of up to 86% when mapping four grassland use intensity classes based on five RapidEye scenes. Bargiel (2013) reported a maximum producer's accuracy of 76% for the grassland class in a 5-class scenario based on six TerraSAR-X acquisitions. Our results show that employing dense intra-annual time series allows for higher classification accuracy on finer thematic and spatial scale. The more acquisition dates are used, the better the mapping quality. In accordance with Prishchepov et al. (2012), high quality grassland mapping requires as many acquisition dates as possible. We observed this for both of the investigated fundamentally different satellite systems that return rather diverging classification power when only a few scenes are used. Therefore, we believe that, in contrast to the assumption of Feilhauer et al. (2013), high revisit capacity could be more important than sensor characteristics.

Our study agrees with recent work in the agricultural domain that demonstrates the crop monitoring potential of Formosat-2 as the first optical system to provide both high spatial and high temporal resolution (Duchemin et al., 2008; Claverie et al., 2012). Apparently, the trade-off paradigm of using either high temporal or high spatial resolution data (Lambin and Linderman, 2006) has been resolved due to improved system configurations.

Performance comparison

For both RapidEye and TerraSAR-X a very high overall accuracy of >90% (Table 3) is attained. While the performance comparison of the sensor systems investigated in this study appears undecided in general, we observed obvious differences in regard to individual classes: In our 7-class scenario, the best overall results are returned for *Molinion caeruleae* and *Arrhenatheretum elatioris*: more or less sensor and index independent, and extremely high accuracies of >95% without exception. Most certainly, the reason is found in the unique phenological development of these habitats: *Molinion caeruleae* meadows, e.g., adopt a dominant yellow coloring in autumn. Its flowering phase is later than for any other species, which makes it very suitable for observation in optical time series. It is an herbaceous perennial bunchgrass that grows up rather high, has closely packed stems, and a dense tussock (Klapp and von Boberfeld, 1995; Rothmaler, 2000, 2005). This distinct structural development is further characterized by a specific required mowing regime that determines a single hay cut in late summer. For *Arrhenatheretum elatioris*, the vegetation growth phase is even separated into three phases. Two hay cuts are mandatory, the first one not before mid June (BfN, 2011; Schuster et al., 2011). While these two classes may also profit from the relatively high sample size (Table 2), this aspect appears not to be very influential. Following the same argumentation, the results for *C. elatae* could be the overall worst, since this habitat shows a less distinct phenological pattern.

Sensor-specific best results for TerraSAR-X are returned for *Arrhenaterion elatioris* and *S. canadensis*. In these habitats the dominant plants grow up very high and rather quickly, returning a clear structural trajectory in the X-band response. In general, comparably low accuracy is attained for *C. palustris* with their relatively low structural development, in this respect similar to *C. elatae*, where the accuracy is lower than for the optical data. *Caltha palustris* as a perennial herbaceous plant is especially known for its distinct blossoming period (Klapp and von Boberfeld, 1995; Rothmaler, 2000, 2005), which could be a reason for the comparably better performance of the RapidEye optical time series. Particularly good class-specific results for RapidEye are returned for *C. elatae* and *Phragmitetum australis* when the NDVI-NIR-RE is used. Only for these two habitats, a clearly positive red-edge effect is observed. The findings of class-specific red-edge effects confirm previous results by Schuster et al. (2012b). However, neither of the red-edge adaptations outperforms the classic NDVI in general.

Number of image acquisitions

The mapping quality increases with the number of acquisition dates. Findings of previous grassland studies also suggest a general rise in classification accuracy with increasing scene numbers (e.g., Prishchepov et al., 2012). However, the question of how many scenes are ultimately needed is becoming a major issue in remote sensing research as the availability of high temporal resolution data increases. Yet, the relationship between costs and quality standards must be considered (Franke et al., 2012), in particular with respect to operational surveys. For distinguishing crops, accurate maps can be produced with only a few selected scenes from multiple observations (Murakami et al., 2001; Van Niel and McVicar, 2004). Our study indicated that a reduced number of time steps can be sufficient for accurate grassland mapping depending on the data type.

Only six to seven (out of 21) RapidEye scenes led to 85% classification accuracy, in case of TerraSAR-X 13 scenes were necessary. Nevertheless, these numbers only provide a relatively broad indicator of sensor-specific data requirements. In fact, the actual number of scenes needed may vary considerably; in our study, the algorithm may choose the best out of 21 available features. This is advantageous over a study where the algorithm cannot select the best scenes out of so many but must deal with fewer features given *a priori* due to external framework conditions. In addition, the number of scenes actually required depends on the specific mapping target, environmental conditions, and inter-annual variability in phenological development. Thus, it is not possible to infer a recommendation on the actual number of scenes from this study. However, the results give an estimate for the data requirements, also in operational surveys.

Implications of the sensor selection for operational mapping

A recommendation regarding sensor choice for operational habitat mapping cannot be derived clearly; achievable accuracies are very high using both technologies. The difference is in the way this can be achieved. While RapidEye has the important cost-relevant advantage of requiring significantly less data, TerraSAR-X provides better data availability and less pre-processing expenditure. The acquisition of intra-annual time series is much more feasible and reliable using TerraSAR-X. It gathered data in almost constant 11-day periods (in average 12.5 days). Time series acquisition is only interfered by potential order conflicts or data storage limitations. The generation of dense intra-annual time series still remains a major challenge for optical data acquisition. While frequent overall coverage may be achieved, the acquisition is not reliable and long acquisition gaps due to cloudiness occur despite the advanced multitemporal capabilities of RapidEye (this study) or Formosat-2 (Claverie et al., 2012). Due to cloud interference even coarse spatial resolution studies using MODIS 16-day composites lack truly equidistant time series gaps (e.g., Alexandridis et al., 2009; Zhang et al., 2009; Verbesselt et al., 2010). This issue required employing the phenological correction approach introduced by Foerster et al. (2012). Apart from that, the pre-processing of the optical data set requires further additional procedures for each individual scene, like geo-rectification, atmospheric correction, cloud masking and interpolation. It is therefore much more elaborate as compared to the SAR time series, where the data is acquired in homogeneous viewing geometry without atmospheric interference. Thus, when the data are ordered as EEC products, considerably fewer and simpler pre-processing steps must be performed (e.g., geo-referencing applied only once for the entire layer stack).

Suitability of TerraSAR-X time series

In accordance with the expectations of Hill et al. (2005), our results support the observation that, while land-cover classifications are the traditional domain for optical data, radar is advancing with the technical evolution of SAR system configurations. Since the start of TerraSAR-X the usability for vegetation mapping has greatly improved (Lopez-Sanchez et al., 2010; Baghdadi et al., 2010; Bargiel and Herrmann, 2011; Esch et al., 2011). Our study introduces the separability of different habitat types within semi-natural grassland vegetation. It extends previous observations on the sensitivity of X-band data to semi-natural grassland vegetation (Schuster et al., 2011; Ali et al., 2013) and for the classification of grassland and semi-natural vegetation structures in agricultural areas (Bargiel, 2013). Our findings further corroborate early studies concerning the prospective applicability of X-band satellites (Le Toan et al., 1989). They confirm the expectations of Rizzoli et al. (2011), who emphasize the high potential of characterizing the X-band backscatter for different vegetation classes, particularly for the monitoring of X-band backscatter variability with time. In fact, the general strength and advantage of SAR systems, multitemporal reliability because of all-weather capability, is being realized for grassland monitoring in the first place.

Conclusions

Remote sensing based mapping of small-scale semi-natural vegetation habitats is possible. The key, however, is to acquire intra-annual time series from satellites that provide both high spatial and high temporal resolution. Thus, we achieved very high classification accuracies for the humid grassland habitats in our study site, a nature reserve area in northeastern Germany. The challenge of mapping small-extent habitats of high diversity can be met using either optical (RapidEye) or X-band SAR (TerraSAR-X) data. We conclude that not only optical analyses of greenness and brightness information, but also structural–morphological parameters from imaging radar are ultimately indicative of grassland compositions. Using RapidEye, distinctly fewer scenes are required to attain relevant classification accuracy. TerraSAR-X provides more reliable time series acquisition and reduced pre-processing expenditure.

In summary, the achieved classification quality is a prerequisite for operational usage. It enables reliable application for a wide range of grassland and biodiversity monitoring purposes. In particular, mapping the Natura 2000 habitat types 6410 (*M. caeruleae*) and 6510 (*Arrhenatheretum elatioris*) was achieved with >95% overall accuracy for any of the employed feature stacks. Classified as 'highly endangered of extinction' (BfN, 2011), these habitats are of special interest for the extension of remote sensing approaches as part of the Natura 2000 monitoring. Additionally, our results suggest intra-annual TerraSAR-X time series cannot only be used for the detection of mowing events as additional monitoring parameter (Schuster et al., 2011, 2012a), but also for direct pixel-based mapping purposes.

Despite the assumed transferability, other factors such as topography, site-specific ecosystem composition (no and type of classes) and characteristics (area dominance of single species depending on soil conditions, etc.) could affect the performance of the separability study. Thus, e.g., the time steps sufficient for successful separation of grassland classes, can hardly be forecasted. Following on this study, the approach should be applied on different research sites to test its robustness and to extend it to further habitat types.

The overall effort for data collection and proper pre-processing is immense and needs to be reduced in view of operational surveys. Future studies should therefore investigate optimal trade-offs in terms of data requirements and mapping quality. To this end, finding reliable statistical methods to determine optimal acquisition time windows remains a key challenge (Schmidt et al., in review). Also, different ways of synergistic analysis could be evaluated to exploit the complementary advantages of optical and SAR data. Finally, the integration of classification and the mowing regime as management parameter (Schuster et al., 2011) should be investigated to further approach the establishment of comprehensive grassland monitoring schemes.

Acknowledgements

This study was conducted within the CARE-X project (**C**hange Detection **A**nalysis for the Monitoring of Biodiversity in the Framework of the Natura 2000 Directive Utilizing **R**apid**E**ye and TerraSAR-**X** Satellite Data) at the Technical University of Berlin. The project was funded by the German National Space Agency DLR (Deutsches Zentrum für Luft- und Raumfahrt e.V.) on behalf of the German Federal Ministry of Economy and Technology based on the Bundestagresolution 50EE0923. We acknowledge the DLR for the delivery of this outstanding database consisting of RapidEye (Science Archive proposal 319) and TerraSAR-X imagery (Science Archive proposal LAN0685). We thank the nature reserve society Döberitzer Heide e.V. for providing access to the study site and supportive information. Particular thanks go to the team of Luftbild Umwelt Planung GmbH Potsdam, Annett Frick, Kristin Batsch and Anne Clasen, for their extensive field surveys within the project. We further thank Iftikhar Ali, Kristin Fenske and Oscar Fuertes for performing several pre-processing steps, Andreas Rabe for support in imageSVM and several reviewers who helped to improve the manuscript.

References

Alcantara, C., Kuemmerle, T., Prishchepov, A.V., Radeloff, V.C., 2012. Mapping abandoned agriculture with multi-temporal MODIS satellite data. Remote Sens. Environ. 124, 334–347.
Alexandridis, T.J., Lazaridou, E., Tsirika, A., Zalidis, G.C., 2009. Using Earth Observation to update a Natura 2000 habitat map for a wetland in Greece. J. Environ. Manage. 90, 2243–2251.
Ali, I., Schuster, C., Zebisch, M., Förster, M., Kleinschmit, B., Notarnicola, C., 2013. First results of monitoring nature conservation sites in alpine region by using very high resolution, VHR X-Band SAR data. IEEE J. Sel. Top. Appl. Earth Observ. Remote Sens. 6, 2265–2274.
Atzberger, C., Eilers, P.H.C., 2011. A time series for monitoring vegetation activity and phenology at 10-daily time steps covering large parts of South America. Int. J. Digit. Earth 4, 365–386.
Atzberger, C., 2013. Advances in remote sensing of agriculture: context description, existing operational monitoring systems and major information needs. Remote Sens. 5, 949–981.
Baghdadi, N., Boyer, N., Todoroff, P., El Hajj, M., Begue, A., 2009. Potential of SAR sensors TerraSAR-X, ASAR/ENVISAT, and PALSAR/ALOS for monitoring sugarcane crops on Reunion Island. Remote Sens. Environ. 113, 1724–1738.
Baghdadi, N., Cresson, R., Todoroff, P., Moinet, S., 2010. Multitemporal observations of sugarcane by TerraSAR-X images. Sensors 10, 8899–8919.
Bargiel, D., Herrmann, S., 2011. Multi-temporal land-cover classification of agricultural areas in two European regions with high resolution spotlight TerraSAR-X data. Remote Sens. 3, 859–877.
Bargiel, D., 2013. Capabilities of high resolution satellite radar for the detection of semi-natural habitat structures and grasslands in agricultural landscapes. Ecol. Inform. 13, 9–16.
Baumann, M., Ozdogan, M., Kuemmerle, T., Wendland, K.J., Esipova, E., Radeloff, V.C., 2012. Using the Landsat record to detect forest-cover changes during and after the collapse of the Soviet Union in the temperate zone of European Russia. Remote Sens. Environ. 124, 174–184.
BfN, Federal Agency for Nature Conservation, 2011. Natura 2000 Habitats in Germany, http://www.bfn.de/0316_typ_lebensraum+M5054de7a952.html (accessed 30.03.11).
Bock, M., Xofis, P., Mitchley, J., Rossner, G., Wissen, M., 2005. Object-oriented methods for habitat mapping at multiple scales – case studies from Northern Germany and Wye Downs, UK. J. Nat. Conserv. 13, 75–89.
Boyd, D.S., Almond, S., Dash, J., Curran, P.J., Hill, R.A., 2011. Phenology of vegetation in Southern England from Envisat MERIS terrestrial chlorophyll index (MTCI) data. Int. J. Remote Sens. 32, 8421–8447.
Breit, H., Fritz, T., Balss, U., Lachaise, M., Niedermeier, A., Vonavka, M., 2010. TerraSAR-X SAR processing and products. IEEE Trans. Geosci. Remote Sens. 48, 727–740.
Chan, J.C.-W., Beckers, P., Spanhove, T., Vanden Borre, J., 2012. An evaluation of ensemble classifiers for mapping Natura 2000 heathland in Belgium using spaceborne angular hyperspectral (CHRIS/Proba) imagery. Int. J. Appl. Earth Observ. Geoinf. 18, 13–22.
Claverie, M., Demarez, V., Duchemin, B., Hagolle, O., Ducrot, D., Marais-sicre, C., Dejoux, J., 2012. Maize and sunflower biomass estimation in southwest France using high spatial and temporal resolution remote sensing data. Remote Sens. Environ. 124, 844–857.
Congalton, R.G., Green, K., 2009. Assessing the Accuracy of Remotely Sensed Data: Principles and Practices, 2nd ed. CRC Press, Florida.
Conrad, C., Machwitz, M., Schorcht, G., Löw, F., Fritsch, S., Dech, S., 2011. Potentials of RapidEye time series for improved classification of crop rotations in heterogeneous agricultural landscapes: experiences from irrigation systems in Central Asia. In: Proceedings of SPIE, 8174, Prague, Czech Republic.
Conrad, C., Fritsch, S., Lex, S., Löw, F., Rücker, G., Schorcht, G., Sultanov, M., 2012. Potenziale des Red Edge Kanals von RapidEye zur Unterscheidung und zum Monitoring landwirtschaftlicher Anbaufrüchte am Beispiel des usbekischen Bewässerungssystems Khorezm. In: Borg, E., Daedelow, H., Johnson, R. (Eds.), RapidEye Science Archive (RESA) – Vom Algorithmus zum Produkt, 4. RESA Workshop. GITO mbH Verlag, Berlin, pp. 203–217.
De Bello, F., Lavorel, S., Gerhold, P., Reier, Ü., Pärtel, M., 2010. A biodiversity monitoring framework for practical conservation of grasslands and shrublands. Biol. Conserv. 143, 9–17.
Dierschke, H., 1994. Pflanzensoziologie: Grundlagen und Methoden. Ulmer, Stuttgart.
Duchemin, B., Hagolle, O., Mougenot, B., Benhadj, I., Hadria, R., Simonneaux, V., Ezzahar, J., Hoedjes, J., Khabba, S., Kharrou, M.H., Boulet, G., Dedieu, G., Er-Raki, S., Escadafal, R., Olioso, A., Chehbouni, A.G., 2008. Agrometerological study of semi-arid areas: an experiment for analysing the potential of time series of FORMOSAT-2 images (Tensift-Marrakech plain). Int. J. Remote Sens. 29, 5291–5300.
Esch, T., Schenk, A., Ullmann, T., Thiel, M., Roth, A., Dech, S., 2011. Characterization of land cover types in TerraSAR-X images by combined analysis of speckle statistics and intensity information. IEEE Trans. Geosci. Remote Sens. 46, 1911–1925.
Esch, T., Metz, A., Marconcini, M., Keil, M., 2014. Combined use of multi-seasonal high and medium resolution satellite imagery for parcel-related mapping of cropland and grassland. J. Appl. Earth Observ. Geoinf. 28, 230–237.
European Commission, 2005. Note to the Habitats Committee: Assessment, Monitoring and Reporting of Conservation Status – Preparing the 2001–2007 Report under Article 17 of the Habitats Directive. DocHab-04-03/03 rev.3. European Commission, Brussels.
Evans, T.L., Costa, M., 2013. Landcover classification of the Lower Nhecolândia subregion of the Brazilian Pantanal Wetlands using ALOS/PALSAR, RADARSAT-2 and ENVISAT/ASAR imagery. Remote Sens. Environ. 128, 118–137.
Feilhauer, H., Thonfeld, F., Faude, U., He, K.S., Rocchinie, D., Schmidtlein, S., 2013. Assessing floristic composition with multispectral sensors – a comparison based on monotemporal and multiseasonal field spectra. Int. J. Appl. Earth Observ. Geoinf. 21, 218–229.
Foerster, M., Frick, A., Walentowski, H., Kleinschmit, B., 2008. Approaches to utilising Quickbird-data for the monitoring of Natura 2000 habitats. Community Ecol. 9, 155–168.
Foerster, S., Kaden, K., Foerster, M., Itzerott, S., 2012. Crop type mapping using spectral–temporal profiles and phenological information. Comput. Electron. Agric. 89, 30–40.
Fontana, F., Rixen, C., Jonas, T., Aberegg, G., Wunderle, S., 2008. Alpine grassland phenology as seen in AVHRR, VEGETATION, and MODIS NDVI time series – a comparison with in situ measurements. Sensors 8, 2833–2853.
Foody, G.M., Mathur, A., 2004. A relative evaluation of multiclass image classification by support vector machines. IEEE Trans. Geosci. Remote Sens. 6, 1335–1343.
Foody, G.M., Mathur, A., Sanchez-Hernandez, C., Boyd, D.S., 2006. Training set size requirements for the classification of a specific class. Remote Sens. Environ. 104, 1–14.
Foody, G.M., 2008. Harshness in image classification accuracy assessment. Int. J. Remote Sens. 29, 3137–3158.
Franke, J., Keuck, V., Siegert, F., 2012. Assessment of grassland use intensity by remote sensing to support conservation schemes. J. Nat. Conserv. 20, 125–134.
Gitelson, A., Merzlyak, M.N., 1994. Spectral reflectance changes associated with autumn senescence features and relation to chlorophyll estimation. J. Plant Physiol. 143, 286–292.
Griffiths, P., Hostert, P., Gruebner, O., van der Linden, S., 2010. Mapping megacity growth with multi-sensor data. Remote Sens. Environ. 114, 426–439.
Gu, Y., Brown, J.F., Miura, T., van Leeuwen, W.J.D., Reed, B.C., 2010. Phenological classification of the United States: a geographic framework for extending multi-sensor time-series data. Remote Sens. 2, 526–544.
Hadria, R., Duchemin, B., Jarlan, L., Dedieu, G., Baup, F., Khabba, S., Olioso, A., Le Toan, T., 2010. Potentiality of optical and radar satellite data at high spatio-temporal resolutions for the monitoring of irrigated wheat crops in Morocco. Int. J. Appl. Earth Observ. Geoinf. 12, 32–37.
Halder, A., Ghosh, A., Ghosh, S., 2009. Aggregation pheromone density based pattern classification. Fundamenta Informaticae 92, 345–362.
Hill, M.J., Donald, G.E., Vickery, P.J., 1999. Relating radar backscatter to biophysical properties of temperate perennial grassland. Remote Sens. Environ. 67, 15–31.
Hill, M.J., Ticehurst, C.J., Lee, J., Fellow, L., Grunes, M.R., Donald, G.E., Henry, D., 2005. Integration of optical and radar classifications for mapping pasture type in Western Australia. IEEE Trans. Geosci. Remote Sens. 43, 1665–1681.

Huang, C., Davis, L.S., Townshend, J.R., 2002. An assessment of support vector machines for land cover classifications. Int. J. Remote Sens. 23, 725–749.

Infoterra, 2008. TerraSAR-X Ground Segment. Level 1B Product Format Specifications, http://www2.astrium-http://www2.astrium-geo.com/files/pmedia/public/r460_9_030201_level-1b-product-format-specification_1.3.pdf (accessed 30.06.12).

Jacquin, A., Sheeren, D., Lacombe, J.-P., 2010. Vegetation cover degradation assessment in Madagascar savanna based on trend analysis of MODIS NDVI time series. Int. J. Appl. Earth Observ. Geoinf. 12, 3–10.

Jong-Sen, L., Grunes, M.R., de Grandi, G., 1999. Polarimetric SAR speckle filtering and its implication for classification. IEEE Trans. Geosci. Remote Sens. 37, 2363–2373.

Justice, C.O., Hiernaux, P.H.Y., 1983. Monitoring the grasslands of the Sahel using NOAA AVHRR data: Niger 1983. Int. J. Remote Sens. 7, 1475–1497.

Klapp, E., von Boberfeld, W.O., 1995. Gräserbestimmungsschlüssel für die häufigsten Grünland-und Rasengräser. Zur Ansprache im blütenlosen Zustand, 4th ed. Blackwell, Berlin.

Klimek, S., Richter, A., Hofmann, M., Isselstein, J., 2007. Plant species richness and composition in managed grasslands: the relative importance of field management and environmental factors. Biol. Conserv. 134, 559–570.

Kohavi, R., John, G.H., 1997. Wrappers for feature subset selection. Artif. Intell. 97, 273–324.

Lambin, E.F., Linderman, M., 2006. Time series of remote sensing data for land change science: geoscience and remote sensing. IEEE Trans. Geosci. Remote Sens. 44, 1926–1928.

Laurin, G.V., Liesenberg, V., Chen, Q., Guerriero, L., Del Frate, F., Bartolini, A., Coomes, D., Wilebore, B., Lindsell, J., Valentini, R., 2013. Optical and SAR sensor synergies for forest and land cover mapping in a tropical site in West Africa. Int. J. Appl. Earth Observ. Geoinf. 21, 7–16.

Le Toan, T., Laur, H., Mougin, E., Lopes, A., 1989. Multi-temporal and dual-polarization observations of agricultural vegetation covers by X-band SAR images. IEEE Trans. Geosci. Remote Sens. 27, 709–718.

Lhermitte, S., Verbesselt, J., Verstraeten, W.W., Coppin, P., 2011. A comparison of time series similarity measures for classification and change detection of ecosystem dynamics. Remote Sens. Environ. 115, 3129–3152.

Lopez-Sanchez, J.M., Ballester-Berman, J.D., Hajnsek, I., 2010. First results of rice monitoring practices in Spain by means of time series of TerraSAR-X dual-pol images. IEEE J. Sel. Top. Appl. Earth Observ. Remote Sens. 4, 412–422.

Mehner, H., Cutler, M., Fairbairn, D., Thompson, G., 2004. Remote sensing of upland vegetation: the potential of high spatial resolution satellite sensors. Glob. Ecol. Biogeogr. 13, 359–369.

Morán-Ordónez, A., Suárez-Seoane, S., Elith, J., Calvo, L., de Luis, E., 2012. Satellite surface reflectance improves habitat distribution mapping: a case study on heath and shrub formations in the Cantabrian Mountains (NW Spain). Divers. Distrib. 18, 588–602.

Moreau, S., Le Toan, T., 2003. Biomass quantification of Andean Wetland forages using ERS SAR data. Remote Sens. Environ. 84, 477–492.

Mountrakis, G., Im, J., Ogole, C., 2010. Support vector machines in remote sensing: a review. ISPRS J. Photogramm. Remote Sens. 66, 247–259.

Murakami, T., Ogawa, S., Ishitsuka, N., Kumagai, K., Saito, G., 2001. Crop discrimination with multitemporal SPOT/HRV data in the Saga Plains, Japan. Int. J. Remote Sens. 22, 1335–1348.

Naeem, S., Duffy, E., Zavaleta, E., 2012. The functions of biological diversity in an age of extinction. Science 336, 1401–1406.

Pott, R., 1995. Die Pflanzengesellschaften Deutschlands, 2nd ed. Ulmer, Stuttgart.

Price, K.P., Guo, X., Stiles, J.M., 2002. Comparison of Landsat TM and ERS-2 SAR data for discriminating among grassland types and treatments in eastern Kansas. Comput. Electron. Agric. 37, 157–171.

Prishchepov, A.V., Radeloff, V.C., Dubinin, M., Alcantara, C., 2012. The effect of Landsat ETM/ETM+ image acquisition dates on the detection of agricultural land abandonment in Eastern Europe. Remote Sens. Environ. 126, 195–209.

Rabe, A., van der Linden, S., Hostert, P., 2010a. Simplifying Support Vector Machines for classification of hyperspectral imagery and selection of relevant features. In: 2nd Workshop of Hyperspectral Image and Signal Processing: Evolution in Remote Sensing, WHISPERS, Reykjavik.

Rabe, A., van der Linden, S., Hostert, P., 2010b. imageSVM, Version 2.1, Available at: www.hu-geomatics.de

Ramoelo, A., Skidmore, A.K., Cho, M.A., Schlerf, M., Mathieu, R., Heitkönig, I.M.A., 2012. Regional estimation of savanna grass nitrogen using the red-edge band of the spaceborne RapidEye sensor. Int. J. Appl. Earth Observ. Geoinf. 19, 151–162.

RapidEye AG, 2012. Satellite Imagery Product Specifications, http://www.rapideye.com/upload/RE_Product_Specifications_ENG.pdf (accessed 14.01.13).

Richter, R., 1996. A spatially adaptive fast atmospheric correction algorithm. Int. J. Remote Sens. 17, 1201–1214.

Rizzoli, P., Bräutigam, B., Wollstadt, S., Mittermayer, J., 2011. Radar backscatter mapping using TerraSAR-X. IEEE Trans. Geosci. Remote Sens. 49, 3538–3547.

Rothmaler, W., 2000. In: Von Rothmaler, W., Jäger, E., Werner, K. (Eds.), Exkursionsflora von Deutschland. Band 3: Gefäßpflanzen: Atlasband. , 10th ed. Spektrum Akademischer Verlag, Heidelberg.

Rothmaler, W., 2005. In: Von Rothmaler, W., Jäger, E., Werner, K. (Eds.), Exkursionsflora von Deutschland. Band 2: Gefäßpflanzen: Grundband. , 19th ed. Spektrum Akademischer Verlag, Heidelberg.

Schmidt, T., Schuster, C., Kleinschmit, B., Förster, M., 2014. Evaluating significant influences on classification accuracy of an intra-annual time-series of semi-natural grassland – how many acquisitions and what seasonal origin are optimal? Sel. Top. Appl. Earth Observ. Remote Sens., In review.

Schmidtlein, S., Zimmermann, P., Schüpferling, R., Weiß, C., 2007. Mapping the floristic continuum: ordination space position estimated from imaging spectroscopy. J. Veg. Sci. 18, 131–140.

Scholes, R.J., Mace, G.M., Turner, W., Geller, G.N., Jürgens, N., Larigauderie, A., Muchoney, D., Walther, B.A., Mooney, H.A., 2008. Toward a global biodiversity observing system. Science 321, 1044–1045.

Schubert, R., Hilbig, H., Klatz, S., 2001. Bestimmungsbuch der Pflanzengesellschaften Deutschlands. Spektrum Akademischer Verlag, Heidelberg.

Schuster, C., Ali, I., Lohmann, P., Frick, A., Förster, M., Kleinschmit, B., 2011. Towards detecting swath events in TerraSAR-X time series to establish Natura 2000 grassland habitat swath management as monitoring parameter. Remote Sens. 3, 1308–1322.

Schuster, C., Ali, I., Lohmann, P., Frick, A., Förster, M., Kleinschmit, B., 2012a. Correction on Towards Detecting Swath Events in TerraSAR-X Time Series to Establish NATURA 2000 Grassland Habitat Swath Management as Monitoring Parameter. Remote Sens. 4, 2455–2456.

Schuster, C., Förster, M., Kleinschmit, B., 2012b. Testing the red edge channel for improving land-use classifications based on high-resolution multi-spectral satellite data. Int. J. Remote Sens. 33, 5583–5599.

Sims, D.A., Gamon, J.A., 2002. Relationships between leaf pigment content and spectral reflectance across a wide range of species, leaf structures and developmental stages. Remote Sens. Environ. 81, 337–354.

Souza, A.A., Galvãog, L.S., Santos, J.R., 2010. Relationships between Hyperion-derived vegetation indices, biophysical parameters, and elevation data in a Brazilian savannah environment. Remote Sens. Lett. 1, 55–64.

Spanhove, T., Vanden Borre, J., Delalieux, S., Haest, B., Paelinckx, D., 2012. Can remote sensing estimate fine-scale quality indicators of natural habitats? Ecol. Indic. 18, 403–412.

Sullivan, C.A., Sheehy Skeffington, M., Gormally, M.J., Finn, J.A., 2010. The ecological status of grasslands on lowland farmlands in western Ireland and implications for grassland classification and nature value assessment. Biol. Conserv. 143, 1529–1539.

Tigges, J., Lakes, T., Hostert, P., 2013. Urban vegetation classification: benefits of multitemporal RapidEye satellite data. Remote Sens. Environ. 136, 66–75.

Tilman, D., Socolow, R., Foley, J., Hill, J., Larson, E., Lynd, L., Pacala, S., Reilly, J., Searchinger, T., Sommerville, C., Williams, R., 2009. Beneficial biofuels – the food, energy, and environment trilemma. Science 325, 270–271.

Tucker, C.J., 1979. Red and photographic infrared linear combinations for monitoring vegetation. Remote Sens. Environ. 8, 127–150.

Ullah, S., Si, Y., Schlerf, M., Skidmore, A.K., Shafique, M., Iqbal, I.A., 2012. Quantifying the biomass and nitrogen of a grassland ecosystem and at regional scale using MERIS data: estimation of grassland biomass and nitrogen using MERIS data. Int. J. Appl. Earth Observ. Geoinf. 19, 196–204.

Van der Linden, S., Hostert, P., 2009. The influence of urban surface structures on the accuracy of impervious area maps from airborne hyperspectral data. Remote Sens. Environ. 113, 2298–2305.

Vanden Borre, J., Paelinckx, D., Mücher, C.A., Kooistra, L., Haest, B., De Blust, G., Schmidt, A.M., 2011. Integrating remote sensing in Natura 2000 habitat monitoring: prospects on the way forward. J. Nat. Conserv. 19, 116–125.

Van Niel, T.G., McVicar, T.R., 2004. Determining temporal windows for crop discrimination with remote sensing: a case study in south-eastern Australia. Comput. Electron. Agric. 45, 91–108.

Verbesselt, J., Hyndman, R., Newnham, G., Culvenor, D., 2010. Detecting trend and seasonal changes in satellite image time series. Remote Sens. Environ. 114, 106–115.

Waske, B., Van der Linden, S., 2008. Classifying multilevel imagery from SAR and optical sensors by decision fusion. IEEE Trans. Geosci. Remote Sens. 46, 1457–1466.

Wright, C.K., Wimberly, M.C., 2013. Recent land use change in the Western Corn Belt threatens grasslands and wetlands. Proc. Natl. Acad. Sci. U. S. A., http://dx.doi.org/10.1073/pnas.1215404110.

Zhang, X., Friedl, M.A., Schaaf, C.B., Strahler, A.H., Hodges, J.C.F., Gao, F., Reed, B.C., 2003. Monitoring vegetation phenology using MODIS. Remote Sens. Environ. 84, 471–475.

Zhang, X., Friedl, M.A., Schaaf, C.B., 2009. Sensitivity of vegetation phenology detection to the temporal resolution of satellite data. Int. J. Remote Sens. 30, 2061–2074.